Biosensors and Bioelectronics 74 (2015) 406–410

Contents lists available at ScienceDirect

Biosensors and Bioelectronics

journal homepage: www.elsevier.com/locate/bios

A nanocoaxial-based electrochemical sensor for the detection of cholera toxin

Michelle M. Archibald [a], Binod Rizal [b], Timothy Connolly [a], Michael J. Burns [b], Michael J. Naughton [b], Thomas C. Chiles [a,*]

[a] Department of Biology, Boston College, Chestnut Hill, MA 02467, United States
[b] Department of Physics, Boston College, Chestnut Hill, MA 02467, United States

ARTICLE INFO

Article history:
Received 9 May 2015
Accepted 26 June 2015
Available online 2 July 2015

Keywords:
Nanocoax
Electrochemistry
DPV
Cholera
Point-of-care
ELISA

ABSTRACT

Sensitive, real-time detection of biomarkers is of critical importance for rapid and accurate diagnosis of disease for point of care (POC) technologies. Current methods do not allow for POC applications due to several limitations, including sophisticated instrumentation, high reagent consumption, limited multiplexing capability, and cost. Here, we report a nanocoaxial-based electrochemical sensor for the detection of bacterial toxins using an electrochemical enzyme-linked immunosorbent assay (ELISA) and differential pulse voltammetry (DPV) or square wave voltametry (SWV). The device architecture is composed of vertically-oriented, nanoscale coaxial electrodes in array format ($\sim 10^6$ coaxes per square millimeter). The coax cores and outer shields serve as integrated working and counter electrodes, respectively, exhibiting a nanoscale separation gap corresponding to $\sim$100 nm. Proof-of-concept was demonstrated for the detection of cholera toxin (CT). The linear dynamic range of detection was 10 ng/ml–1 μg/ml, and the limit of detection (LOD) was found to be 2 ng/ml. This level of sensitivity is comparable to the standard optical ELISA used widely in clinical applications, which exhibited a linear dynamic range of 10 ng/ml–1 μg/ml and a LOD of 1 ng/ml. In addition to matching the detection profile of the standard ELISA, the nanocoaxial array provides a simple electrochemical readout and a miniaturized platform with multiplexing capabilities for the simultaneous detection of multiple biomarkers, giving the nanocoax a desirable advantage over the standard method towards POC applications.

1. Introduction

The development of highly specific and sensitive diagnostic platforms for clinically relevant protein biomarkers is essential in enabling accurate disease detection and monitoring. Emerging and re-emerging infectious diseases constitute some of the most significant public health challenges facing the global community. For example, cholera continues to inflict high rates of mortality in resource limited areas (Dick et al., 2012; Harris et al., 2012) and Ebola outbreaks with extremely high mortality rates present a challenge to even the most sophisticated medical establishments (Center for Disease Control and Prevention, 2014). Current diagnostic devices fail to provide critically-needed capabilities, such as real-time, simultaneous detection of multiple infectious disease markers, and ease of deployment in low resource POC settings. These capabilities are essential in any diagnostic device for surveillance, confirmation, and timely implementation of preventive and protective public health measures. Highly sensitive and specific POC technologies could facilitate better prevention and earlier response, and would be ideally suited for laboratory-free environments as well as in a clinical setting.

ELISA is the most commonly-used method for clinical protein biomarker detection (Lequin, 2005). However, cost and the need for complex instrumentation required for the ELISA measurement limit its potential for POC applications. Microarrays and LC–MS-based proteomics provide alternative platforms to ELISA-based methods. While both technologies are highly sensitive and allow for multiplexing, they also require complex instrumentation and specialized consumables (Aebersold and Mann, 2003; Berrade et al., 2011; Hawkridge, Muddiman, 2009; Lee et al., 2008; Rusling et al., 2010). As a consequence, there remains an unmet need for a rapid, highly sensitive, low-cost biomarker detection platform that would require minimal instrumentation and afford multiplexing capabilities.

Electrochemical-based detection strategies may provide a solution to current challenges associated with many existing methods. Electrochemical sensors have shown the potential to achieve sensitive and specific detection of biomarkers at low-cost and in

* Corresponding author. Fax: +1 617 552 2011.
E-mail address: chilest@bc.edu (T.C. Chiles).

http://dx.doi.org/10.1016/j.bios.2015.06.069
0956-5663/

real-time (Chikkaveeraiah et al., 2012; Sage et al., 2014). The development and commercial success of electrochemical glucose sensor strips for blood sugar monitoring in diabetic patients demonstrates the low-cost and portability of such an electrochemical-based POC technology (Newman and Turner, 2005). Moreover, using electrochemical detection strategies in conjunction with nanostructured electrode surfaces – such as carbon nanotubes (Wang, 2005), silicon nanowires (Wanekaya et al., 2006) and metallic nanoparticles (Luo et al., 2006) – exhibits increased sensitivity for biomarker detection. These nanostructures provide enhanced surface areas for the detection electrodes, significantly improving signal over the standard macroscale electrochemical setup and allowing for increasingly sensitive electrochemical biosensors.

Previously, we developed a novel nanostructure, the nanocoax, resembling a vertically-oriented coaxial electrode on the nanoscale. It consists of two concentric electrodes separated by a dielectric or an air gap. The nanocoax has demonstrated ultrasensitive chemical detection of volatile organic compounds (Zhao et al., 2012) and exhibited nanophotonic properties as a waveguide for visible light (Merlo et al., 2014; Rybczynski et al., 2007). Recently, nanocoaxial arrays demonstrated electrochemical sensing capabilities via the detection of the redox species ferrocenecarboxylic acid (FCA) (Rizal et al., 2013). The nanocoaxial arrays exhibited 90 times greater signal in response to the oxidation of FCA, as compared to their planar counterpart. In addition, a significant improvement in signal-to-noise was observed, as the signal for the nanocoax was approximately 2 orders of magnitude greater than its planar counterpart, while the baseline noise level remained unchanged. Here, we investigate the use of the nanocoax as an electrochemical sensor for the detection of cholera toxin. We report that the nanocoaxial array matches the standard method of protein detection with regard to limit of detection and dynamic range, providing a robust platform for electrochemical detection of infectious diseases with *bona fide* POC prospects.

2. Materials and methods

2.1. Materials

Cholera toxin subunit B (CT), ferrocenecarboxylic acid (FCA) and ethylenediaminetetraacetic acid (EDTA) were purchased from Sigma-Aldrich (St. Louis, MO). All antibodies (Abs) were obtained from Abnova (Taipei, Taiwan). The BluePhos phosphatase substrate system was purchased from KPL (Gaithersburg, MD) and p-aminophenylphosphate (pAPP) was acquired from Gold Biotechnology, Inc. (St. Louis, MO). Bovine serum albumin (BSA), Tween-20, and Tris base were obtained from Fisher Scientific (Pittsburgh, PA). SU-8 was procured from MicroChem Corp. (Westborough, MA) and Transetch-N was obtained from Transene Company, Inc. (Danvers, MA).

2.2. Fabrication of nanocoaxial arrays

SU-8 pillar arrays were fabricated on silicon chips using nanoimprint lithography as previously described (Rizal et al., 2013). A thin film of Au (~125 nm) was deposited onto the SU-8 pillar array via sputter deposition (AJA International, Scituate, MA). Atomic layer deposition (Savannah S100, Cambridge Nanotech, Waltham, MA) was then used to deposit ~200 nm Al_2O_3, followed by a sputter deposition of Cr (~150 nm). A layer of SU-8 was spin-coated on top of the coaxial array and was cured by UV exposure (12 mW/cm^2; 90 s), followed by a hard bake at 200 °C for 1 h. A mechanical polisher was used to remove the top part of the outer Cr of the coax array using an alumina slurry for 2.5 h. This mechanical decapitation of the coax exposed the Al_2O_3 in the coaxes' annuli, allowing for wet etching of the Al_2O_3 with Transetch-N to form an annulus cavity approximately 500 nm deep. Of note, arrays were stored dry at room temperature for up to one year until further use, with no notable degradation of performance.

2.3. ELISA

The wells of a 96-well plate were coated with 1 μg/ml of anti-cholera toxin antibody (anti-CT Ab) in 0.1 M $NaHCO_3$, pH 9.6 for 2 h at room temperature. The solution was removed from the plate and the wells were washed three times with TBST (0.05% Tween-20, 50 mM Tris, 150 mM NaCl, pH 7.4); the wells were blocked with 5% BSA in TBST overnight at 4 °C. Next, several different concentrations of CT antigen in 2% BSA/TBST were added to each well and incubated for 1 h at room temperature. The plate was then washed three times with TBST. A second anti-CT Ab was added to each well at a concentration of 50 ng/ml in 2% BSA/TBST for 1 h at room temperature. The plate was washed three times with TBST. Anti-mouse IgG alkaline phosphatase labeled Ab was added to each well at a dilution of 2.7 μg/ml in 2% BSA/TBST for 1 h at room temperature. The plate was washed six times with TBST. Lastly, the wells were incubated with 1 mM pAPP in TBS reaction buffer (50 mM Tris, 1 mM $MgCl_2$, pH 9.0) at room temperature in the dark. The reaction was stopped after 30 min by adding 40 μl of 50 mM EDTA in TBS to each well. The solution from each of the wells was then pipetted onto the nanocoaxial array for electrochemical measurements.

2.4. Electrochemical ELISA readout

All electrochemical readouts were carried out on a Reference 600 potentiostat (Gamry Instruments, Warminster, PA) using a three-electrode system. An external Ag/AgCl wire served as the reference electrode. The outer Cr of the nanocoaxes in the array served as the counter electrode and the inner Au of the nanocoaxes functioned as the working electrode. DPV was used as the method for ELISA electrochemical readout. DPV measurements were performed using the potential range of −0.5 V to 0.4 V, a potential step of 2 mV, a pulse amplitude of 50 mV, a pulse width of 50 ms, a pulse sample period of 100 ms, and an equilibrium time of 10 s.

2.5. Optical ELISA readout

Optical ELISAs were performed in the exact same manner alongside electrochemical ELISAs, except that the BluePhos phosphatase substrate system replaced pAPP in the final step of the assay. BluePhos was chosen over the traditional pNPP optical substrate due to its greater sensitivity. The reaction was stopped after 30 min by adding 40 μl of 50 mM EDTA to each well. Optical absorbance was measured spectroscopically at 600 nm on a SpectraMax M5 (Molecular Devices, Sunnyvale, CA).

3. Results

In order to fabricate the nanocoaxial sensor, nanoimprint lithography was used to construct the base SU-8 pillar array on a silicon substrate. Nanoimprint lithography is a rapid and cost-effective method for producing a large number of replicas from a single master, and is optimal for 3D nanostructures such as the vertical pillar arrays used here (Guo, 2007). Fabrication of the nanocoaxial arrays is depicted schematically in Fig. 1a. Successful fabrication of nanocoaxial arrays were confirmed with SEM

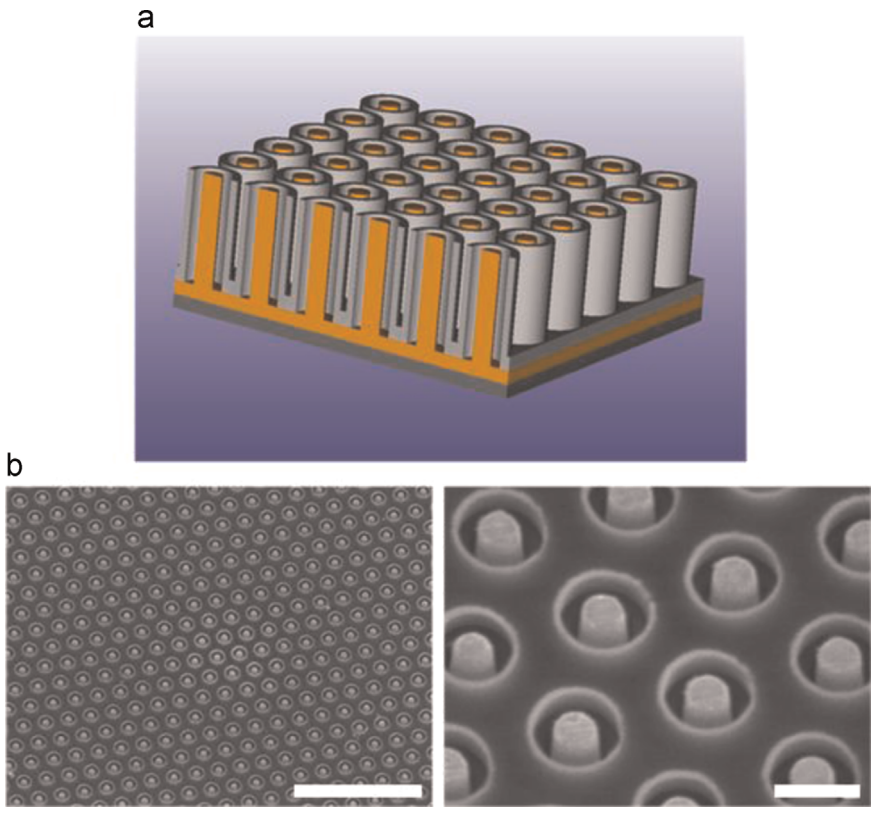

Fig. 1. Structure of the nanocoax. (a) Schematic representation of a nanocoaxial array with an etched annulus. The inner Au core (shown in orange) serves as the working electrode (WE) and the outer Cr metal (gray) serves as the counter electrode (CE). (b) SEM images of an array with 150 nm annulus thickness and 500 nm annulus depth with inner Au and outer Cr electrodes. Volume between individual coaxes is filled with SU-8 polymer. Scale bars represent 5 μm length (left image) and 500 nm length (right image). (For interpretation of the references to color in this figure legend,the reader is referred to the web version of this article.)

(Fig. 1b). All arrays had a base area of 1.8 mm^2 and contained $\sim 10^6$ individual nanocoaxes electrically connected in parallel. To confirm electrical integrity of each nanocoaxial array, resistance was measured between the working electrode and the counter electrode of each array (data not shown). Typical resistance values of devices used ranged from 10–100 GΩ. Nanocoaxial arrays were additionally tested with the redox species FCA to confirm electrochemical sensing capabilities, with an average initial peak current of approximately -100 μA.

To evaluate the use of the nanocoaxial array as a potential biosensor, DPVs of an alkaline phosphatase (ALP) titration were examined for proof-of-concept of an electrochemical ELISA. DPV was chosen as the method for electrochemical analysis due to its suppression of background current and its previously reported sensitive and reliable detection of ALP activity (Ricci et al., 2012). In addition, we analyzed ALP titrations using square wave voltammetry (SWV) and compared these data to that of parallel measurements with DPV (Figs. S1 and S2). We found that the dynamic range and LOD as measured by SWV were comparable to that of DPV. Serial dilutions of ALP were incubated with 1 mM of the enzymatic substrate 4-aminophenolphosphate (pAPP) and then electrochemically examined on the nanocoax (Fig. 2a), as well as on a planar gold counterpart (Fig. 2b). Each set of titration data (nanocoax and planar) was taken on a single device. Runs on additional devices gave qualitatively similar results, however it is noted that some devices exhibited no electrochemical signal, likely due to fabrication issues. ALP converts pAPP into the electrochemical reporter product 4-aminophenol (4AP), which is subsequently detected upon reaching its oxidation potential at -100 mV during a DPV scan. With the planar gold device, an ALP concentration of 10^{-3} ng/ml was required to measure an appreciable signal change from baseline at the -100 mV region. However, the nanocoax exhibited a noticeable current peak from baseline starting at an ALP concentration of 10^{-6} ng/ml. To determine the detection range, the peak current was normalized to the base area of each sensor and plotted against ALP concentration (Fig. 2c). The planar gold device exhibited lower overall current magnitude compared to the nanocoax. In addition, the nanocoax exhibited a greater log-linear dynamic range, over the ALP concentrations of 10^{-6}–1 ng/ml. The planar counterpart, on the other hand, exhibited only a two decade dynamic range from 10^{-4}–10^{-2} ng/ml ALP, with trending saturation at the upper end and a lower limit of detection at 10^{-4} ng/ml ALP. It is worth noting that the true "active" area of the nanocoaxial array (i.e. the working electrode within each coax) is only a fraction (about 1/4) of the array's base area to which the current was normalized; yet the electrochemical signal from the nanocoax still surpasses that of the planar device whose entire base area constitutes its working electrode. Similar arrays with smaller pitch and deeper etched annuli could have yet higher sensitivity than those presented here. Therefore, this ALP titration highlights not only proof-of-concept for an electrochemical ELISA on the nanocoax, but also the advantage of the nanocoaxial structure over its planar counterpart towards greater electrochemical sensing capabilities.

We next performed an ELISA for electrochemical readout on the nanocoax. CT was chosen as the target protein due to its clinical relevance in water-borne infectious diseases (WHO Cholera, 2012). ELISA reaction supernatants were applied to the nanocoaxial array and DPVs were subsequently recorded. Fig. 3 shows the DPVs obtained for one of the replicates, with the current subtracted to baseline at -0.15 V to elucidate the peak current for each CT concentration. To determine the dynamic range, peak current was plotted against the CT concentration on the log scale (Fig. 4). The data points depicted in Fig. 4 represent two

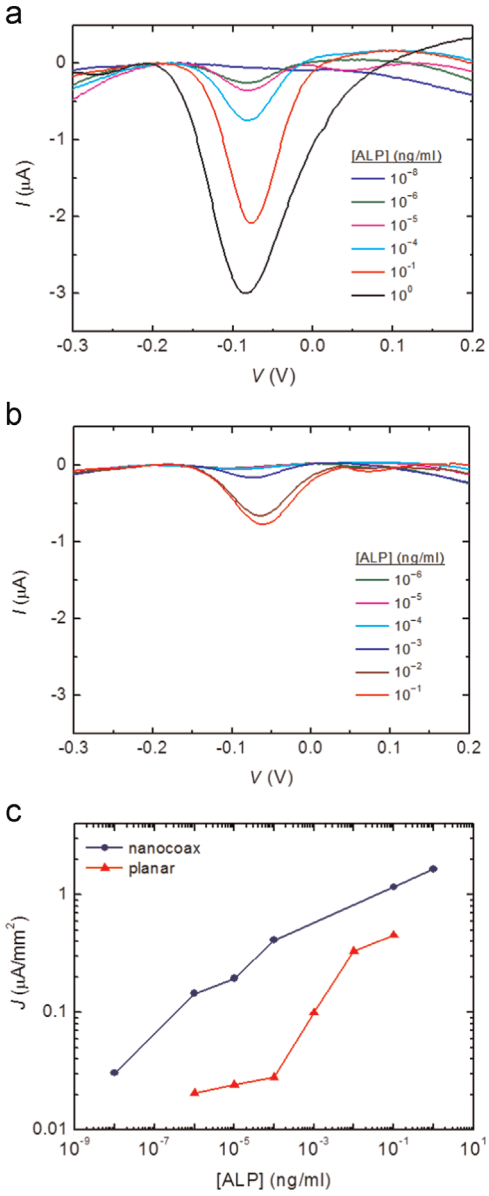

Fig. 2. DPV signal from an ALP dose titration on (a) a nanocoaxial array and (b) a planar Au sensor. DPVs were subtracted to baseline at −0.2 V for both nanocoax and planar samples to determine peak current. (c) Comparison of planar Au and nanocoaxial ALP log-linear range of detection shown by peak current normalized to each sensor base area.

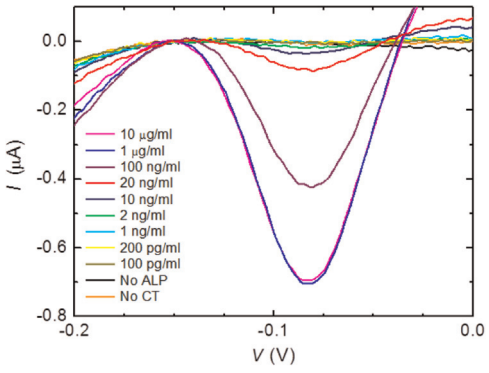

Fig. 3. Electrochemical ELISA for detection of CT by a nanocoaxial array. DPV signals for CT concentrations ranging from 100 pg/ml to 10 μg/ml were examined. DPVs were subtracted to baseline at −0.14 V in order to determine peak current. Data shown represents one replicate.

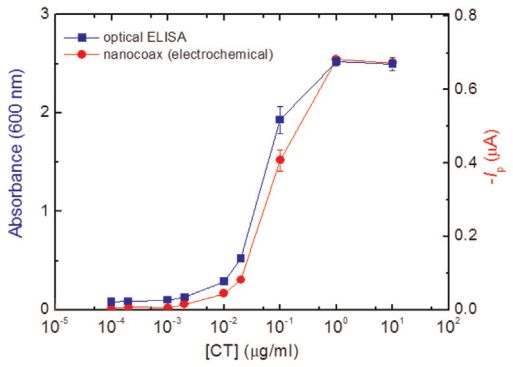

Readout Method	Lower Limit	Linear Dynamic Range
Electrochemical	2 ng/ml	10 ng/ml - 1 μg/ml
Optical	1 ng/ml	10 ng/ml - 1 μg/ml

Fig. 4. Electrochemical and optical readouts of a CT ELISA. On the right *y*-axis, peak current (I_p) vs. CT concentration is plotted for electrochemical detection by the nanocoaxial array (red). Peak currents were determined from the baseline normalized DPV signals as shown in Fig. 3. On the left *y*-axis, absorbance at $\lambda = 600$ nm vs. CT concentration on a log scale for the conventional optical readout of an ELISA (blue). Limit of detection and log-linear dynamic range were determined for each readout method. Data represent two trials run on the same device. Error bars represent standard deviations, however many error bars are smaller than the size of the plotted data points. (For interpretation of the references to color in this figure legend,the reader is referred to the web version of this article.)

ELISA replicates tested on the same nanocoaxial device. Here, we observed a log-linear dynamic range of 10 ng/ml–1 μg/ml, with a lower LOD of 2 ng/ml (as determined by LOD$=I_{p,control}+3\sigma_{control}$; control=No CT sample). Statistical analysis of the replicate data indicates significant reproducibility of measurements on a single nanocoaxial device.

In addition, we compared the electrochemical nanocoaxial sensor to the conventional optical ELISA as a standard control. The optical ELISA was performed in the same manner as the electrochemical ELISA, with the exception that the BluePhos substrate was used in place of pAPP. BluePhos is converted by ALP into a colorimetric product, whose optical absorbance is read at $\lambda_{max}=600$ nm. The optical ELISA was carried out in duplicate and the results are shown in Fig. 4 with CT concentration plotted against absorbance. The optical readout was linear over a dynamic range of 10 ng/ml–1 μg/ml, with a LOD of 1 ng/ml. These results indicate that the nanocoaxial electrochemical sensor is comparable to the standard optical ELISA with respect to the linear dynamic range of detection and LOD (2 ng/ml vs. 1 ng/ml).

4. Discussion

As previously mentioned, the standard optical ELISA is limited in POC applications due to complex instrumentation, high reagent consumption, cost, and lack of facile multiplexing capabilities. The electrochemical readout of an ELISA with the nanocoax matches the standard optical ELISA with regards to CT detection range and LOD, while overcoming a handful of these limitations. The nanocoax architecture allows for a simple electrical readout requiring orders of magnitude less reagent; the active reagent volume in the 1.8 mm^2 arrays employed in the present work was approximately 100 pl. In addition, the architecture allows for facile multiplexing due to the ability to fabricate multiple electrically-independent nanocoaxial arrays on a single chip. Arrays as small as 150 μm^2 have been routinely fabricated, containing only ~100 nanocoaxes and requiring only ~10 fl sample volume. Moreover, the nanoscale proximity of the counter electrode and the working electrode

allows for redox cycling, enhancing the electrochemical signal as compared to the conventional macroscopic system (Rizal et al., 2013). Therefore, the nanocoaxial array offers advantages over the conventional ELISA that make it an attractive candidate for further development towards POC applications.

To be fully realized as a POC device, the detection assay must move away from the plate based format to a "lab-on-a-chip" approach in which capture antibody is immobilized directly onto the coaxial electrode surface. Integration of biomarker capture and electrochemical detection on the nanocoax will allow for a portable and pre-packaged device for POC applications, an option not feasible for the optical ELISA. In addition, integration of the nanocoaxial architecture with electrode functionalization is likely to overcome potential diffusion limitations that may occur with the plate-based assay format and could push the detection range of the nanocoaxial array beyond what is reported here.

5. Conclusion

In summary, we have developed a nanocoaxial electrochemical sensor for the detection of disease biomarkers that, in this initial iteration, matches the current standard method of target protein detection. We have demonstrated that the nanocoaxial array is capable of sensitive detection of CT on par with that of the conventional, widely-used optical ELISA with regard to LOD and dynamic range of detection. The nanocoax architecture offers advantages over the conventional ELISA, providing a simple electrical readout over the non-portable complex instrumentation required for the optical readout, as well as a miniaturized platform that can accommodate several magnitudes smaller sample volume. In addition, the nanocoaxial array could allow for facile multiplexing for the detection of multiple biomarkers simultaneously, whereas multiplexing optical ELISAs proves extremely difficult. In the future, the nanocoax may provide a means for POC detection of disease biomarkers once the assay has moved away from the plate based format to a lab-on-a-chip device, in which biomarker capture has been integrated directly onto the device.

Acknowledgments

This work was supported by the National Cancer Institute Award no. CA137681 and the National Institutes of Allergy and Infectious Disease Award no. AI100216.

Appendix A. Supplementary material

Supplementary data associated with this article can be found in the online version at http://dx.doi.org/10.1016/j.bios.2015.06.069.

References

Aebersold, R., Mann, M., 2003. Mass spectrometry-based proteomics. Nature 422, 198–207. http://dx.doi.org/10.1038/nature01511.
Berrade, L., Garcia, A., Camarero, J., 2011. Protein microarrays: novel developments and applications. Pharm. Res. 28, 1480–1499. http://dx.doi.org/10.1007/s11095-010-0325-1.Protein.
Center for Disease Control and Prevention, 2014. ⟨http://www.cdc.gov/vhf/ebola/⟩.
Chikkaveeraiah, B.V., Bhirde, A.A., Morgan, N.Y., Eden, H.S., Chen, X., 2012. Electrochemical immunosensors for detection of cancer protein biomarkers. ACS Nano 6, 6546–6561. http://dx.doi.org/10.1021/nn3023969.
Dick, M.H., Guillerm, M., Moussy, F., Chaignat, C.-L., 2012. Review of two decades of cholera diagnostics—how far have we really come? PLoS Negl. Trop. Dis. 6, e1845. http://dx.doi.org/10.1371/journal.pntd.0001845.
Guo, L.J., 2007. Nanoimprint lithography: methods and material requirements. Adv. Mater. 19, 495–513. http://dx.doi.org/10.1002/adma.200600882.
Harris, J.B., LaRocque, R.C., Qadri, F., Ryan, E.T., Calderwood, S.B., 2012. Cholera. Lancet 379, 2466–2476. http://dx.doi.org/10.1016/S0140-6736(12)60436-X.
Hawkridge, A.M., Muddiman, D.C., 2009. Mass spectrometry-based biomarker discovery: toward a global proteome index of individuality. Annu. Rev. Anal. Chem. 2, 265–277. http://dx.doi.org/10.1146/annurev.anchem.1.031207.112942.Mass.
Lee, H., Wark, A., Corn, R., 2008. Microarray methods for protein biomarker detection. Analyst 133, 975–983. http://dx.doi.org/10.1039/b717527b.Microarray.
Lequin, R.M., 2005. Enzyme immunoassay (EIA)/enzyme-linked immunosorbent assay (ELISA). Clin. Chem. 51, 2415–2418. http://dx.doi.org/10.1373/clinchem.2005.051532.
Luo, X., Morrin, A., Killard, A.J., Smyth, M.R., 2006. Application of nanoparticles in electrochemical sensors and biosensors. Electroanalysis 18, 319–326. http://dx.doi.org/10.1002/elan.200503415.
Merlo, J., Ye, F., Rizal, B., Burns, M.J., Naughton, M.J., 2014. Near-field observation of light propagation in nanocoax waveguides. Opt. Express 22, 14148–14154. http://dx.doi.org/10.1364/OE.22.014148.
Newman, J.D., Turner, A.P.F., 2005. Home blood glucose biosensors: a commercial perspective. Biosens. Bioelectron. 20, 2435–2453. http://dx.doi.org/10.1016/j.bios.2004.11.012.
Ricci, F., Adornetto, G., Palleschi, G., 2012. A review of experimental aspects of electrochemical immunosensors. Electrochim. Acta 84, 74–83. http://dx.doi.org/10.1016/j.electacta.2012.06.033.
Rizal, B., Archibald, M.M., Connolly, T., Shepard, S., Burns, M.J., Chiles, T.C., Naughton, M.J., 2013. Nanocoax-based electrochemical sensor. Anal. Chem. 85, 10040–10044. http://dx.doi.org/10.1021/ac402441x.
Rusling, J.F., Kumar, C.V., Gutkind, J.S., Patel, V., 2010. Measurement of biomarker proteins for point-of-care early detection and monitoring of cancer. Analyst 135, 2496–2511. http://dx.doi.org/10.1039/c0an00204f.
Rybczynski, J., Kempa, K., Herczynski, A., Wang, Y., Naughton, M.J., Ren, Z.F., Huang, Z.P., Cai, D., Giersig, M., 2007. Subwavelength waveguide for visible light. Appl. Phys. Lett. 90, 021104. http://dx.doi.org/10.1063/1.2430400.
Sage, A.T., Besant, J.D., Lam, B., Sargent, E.H., Kelley, S.O., 2014. Ultrasensitive electrochemical biomolecular detection using nanostructured microelectrodes. Acc. Chem. Res. 47, 2417–2425. http://dx.doi.org/10.1021/ar500130m.
Wanekaya, A.K., Chen, W., Myung, N.V., Mulchandani, A., 2006. Nanowire-based electrochemical biosensors. Electroanalysis 18, 533–550. http://dx.doi.org/10.1002/elan.200503449.
Wang, J., 2005. Carbon-nanotube based electrochemical biosensors: a review. Electroanalysis 17, 7–14. http://dx.doi.org/10.1002/elan.200403113.
WHO Cholera, 2012. ⟨http://www.who.int/mediacentre/factsheets/fs107/en/⟩.
Zhao, H., Rizal, B., McMahon, G., Wang, H., Dhakal, P., Kirkpatrick, T., Ren, Z., Chiles, T.C., Naughton, M.J., Cai, D., 2012. Ultrasensitive chemical detection using a nanocoax sensor. ACS Nano 6, 3171–3178. http://dx.doi.org/10.1021/nn205036e.

Supplementary Information

A Nanocoaxial-Based Electrochemical Sensor for the Detection of Cholera Toxin

Michelle M. Archibald,[1] Binod Rizal,[2] Timothy Connolly,[1] Michael J. Burns,[2] Michael J. Naughton,[2] and Thomas C. Chiles[1]*

[1]Department of Biology, [2]Department of Physics

Boston College, Chestnut Hill, MA 02467

*Corresponding author. Tel: +1 617 552 0840 fax: +1 617 552 2011.

Email address: chilest@bc.edu (Thomas Chiles)

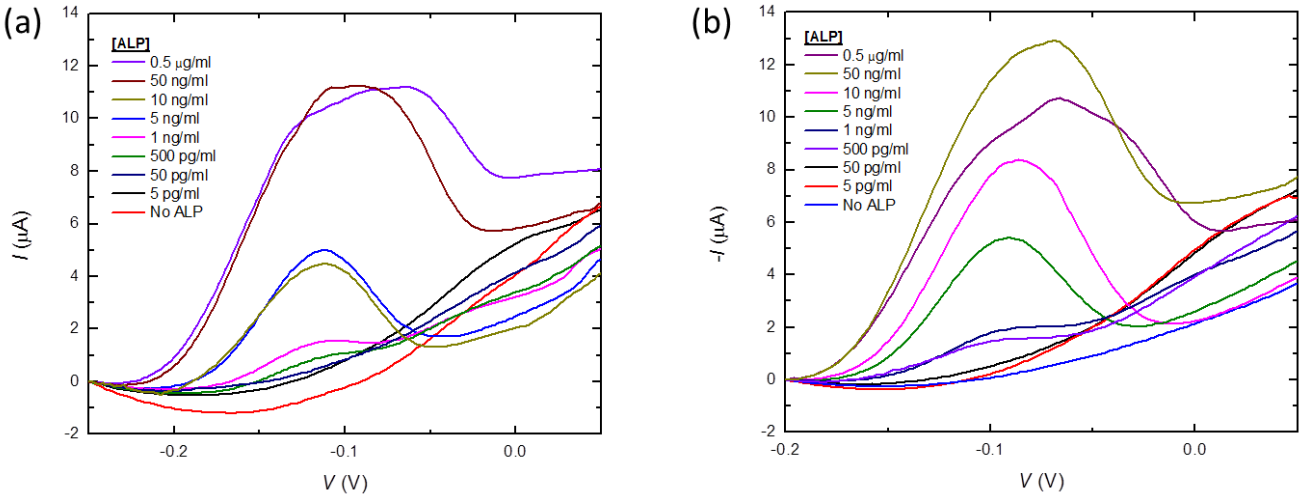

Figure S1. Electrochemical detection of an ALP titration by (a) SWV and (b) DPV on a planar gold electrode. Dilutions of ALP ranging from 5 pg/ml – 0.5 µg/ml were incubated with 1 mM pAPP and the resultant enzymatic product 4-AP was electrochemically detected at -0.1 V. SWV signals were baselined at -0.25 V and DPV signals were baselined at -0.2 V.

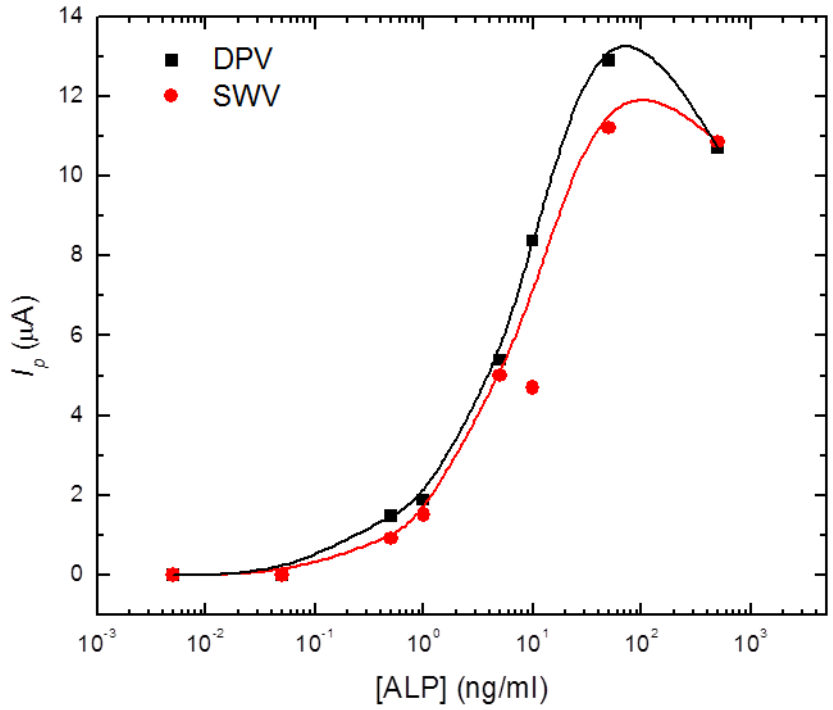

Figure S2. Range of electrochemical detection for ALP by SWV (red) and DPV (black). Peak current (I_p) was plotted against ALP concentration on a log-scale to determine range of detection. Both DPV and SWV exhibit ALP detection over a range of 500 pg/ml to 50 ng/ml. Peak currents were determined from the baseline normalized DPV and SWV signals as shown in Figure S1. Data points were fitted with B-spline curves, excluding the outlier at 10 ng/ml ALP in the SWV curve.